Oxidation Behavior of Atomized Fe40Al Intermetallics Doped with Boron and Reinforced with Alumina Fibers

M.A. Espinosa-Medina, M. Casales, A. Martinez-Villafañe, J. Porcayo-Calderon, G. Izquierdo, L. Martinez, and J.G. Gonzalez-Rodriguez

(Submitted 30 May 2000)

Isothermal oxidation resistance of Fe40 (at.%) Al-based atomized and deposited intermetallic alloys has been evaluated. The alloys included Fe40Al, Fe40Al + 0.1B, and Fe40Al + 0.1B + 10Al_2O_3 at 800, 900, 1000, and 1100 °C. The tests lasted approximately 100 h, although in most cases there was scale spalling. At 800 and 900 °C, the Fe40Al + 0.1B alloy had the lowest weight gain, whereas the Fe40Al alloy had the highest weight gain at 800 °C (0.10 mg/cm^2) and the Fe40Al + 0.1B + 10Al_2O_3 alloy was the least oxidation resistant at 900 °C with 0.20 mg/cm^2. At 1000 °C, the Fe40Al + 0.1B alloy showed the highest weight gain with 0.12 mg/cm^2 and the Fe40Al alloy the lowest. At 1100 °C, again, as at 900 °C, the Fe40Al alloy was the least resistant, whereas the Fe40Al + 0.1B alloy performed the best, but the three alloys exhibited a paralinear bahavior on the weight-gain curves, indicating the spalling, breaking down, and rehealing of the oxides. This spalling was related to voids formed at the metal-oxide interface.

Keywords atomized, iron aluminides, oxidation

1. Introduction

For more than 50 years, iron-aluminum intermetallics have received special interest because of their potentially high oxidation resistance at high temperature.[1] They offer a good alternative for use in automotive parts, chemical processing, and gas turbine technologies since they possess a high melting point, high thermal conductivity, excellent oxidation resistance, low density, and low cost.[2]

Iron aluminides are receiving special attention because they have a good yielding point between 600 and 800 °C, and even up to 1000 °C when they are alloyed with low expansion fibers such as alumina (Al_2O_3).[3] The charpy impact energy is satisfactory at room temperature, and, depending on the grain size, the FeAl (40 at.%) offers a yielding point between 250 and 600 MPa, which can be increased with additions of Hf or B.[4] Also, iron aluminides have a lower density (5.6 g/cm^3) compared with that for stainless steels and some nickel-based alloys, and a relatively high melting point (1237 °C). Their major disadvantage is their poor ductility at room temperature. In the last few years, some new processing routes have been tried to improve their ductility[5] together with the addition of fibers and some microalloying elements.[6] A method that has been used succesfully has been spraying, which avoids macrosegregation and minimizes microsegregation.

The good oxidation resistance of these materials is based on their ability to develop a protective alumina layer (Al_2O_3) on their surface in many high-temperature environments. Because alloys based on Fe_3Al and FeAl form Al_2O_3 during exposure to oxidizing gases, they typically display low oxidation rates when compared to iron-based and other alloys that do not form alumina in similar conditions. Recent studies on Fe_3Al alloys containing 2 to 5 at.% and various minor additions of oxygen-active elements have shown that their long-term oxidation performance approximately matches that of FeCrAlY alloys and NiAl at 1000 °C, but it is inferior at 1200 and 1300 °C.[7,8] Other work has suggested that oxidation of iron aluminides without these oxygen-active elements is worse in air than oxygen, particularly at 1000 and 1100 °C, due to internal nitridation below a defective scale. The Fe_3Al alloys produced by ingot-metallurgy processes tended to have worse oxidation behavior, since they had greater spallation than oxide-dispersion-strengthened iron aluminides of similar composition.[7] In this work, a study of the oxidation behavior of sprayed iron aluminides in oxygen has been carried out.

2. Experimental Procedure

There were three materials employed: Fe40 (at.%) Al, Fe40 (at.%) Al + 0.1 (at.%) B and Fe40 (at.%) Al + 0.1 (at.%) B + 10 (at.%) Al_2O_3. A master alloy of Fe40Al was fabricated employing iron and aluminum, both 99.99% pure. The alloy was cast in an induction furnace under an argon atmosphere and was poured by gravity into a cylindrical graphite mold 4 cm in diameter. Small pieces were cut from the master alloy bar and fed to a spray atomization and deposition system. Boron with a purity of 99.99% in the form of Ni_2B was used as a

M.A. Espinosa-Medina, M. Casales, and **A. Martinez-Villafañe,** CIMAV, Miguel de Cervantes 120, Complejo Ind. Chihuahua, Chihuahua, Chih. Mexico; **J. Porcayo-Calderon** and **G. Izquierdo,** Instituto de Investigaciones Electricas, A.P. 1-62000, Cuernavaca, Mor., Mexico; **L. Martinez**, Centro de Ciencias Fisicas, UNAM, Av. Universidad S.N. Cuernavaca, Mor., Mexico; and **J.G. Gonzalez-Rodriguez**, UAEM, Centro de Inv. en Ingenieria y Ciencias Aplicadas, Av. Universidad 1001, Col. Chamilpa 62210-Cuernavaca, Morelos, Mexico. Both L. Martinez and J.G. Gonzalez-Rodriguez are currently on a sebatic leave at the IMP, Coordinacion de Ductos, Eje Lazaro Cardenaz, Mexico D.F., Mexico. Contact e-mail: ggonzalez@buzon.uaem.mx.

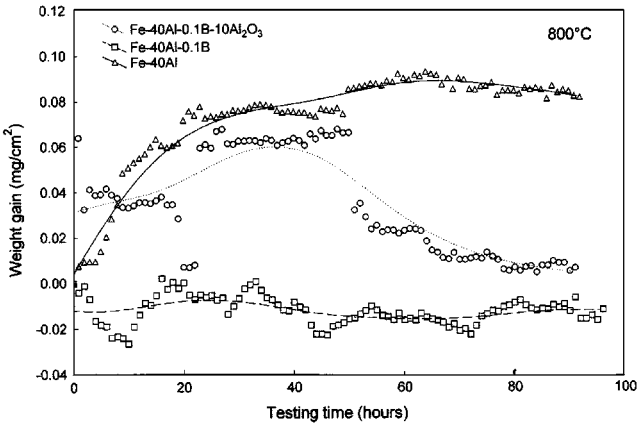

Fig. 1 Gravimetric curves for isothermal oxidation of Fe40Al, Fe40Al + B, and Fe40Al + B + Al_2O_3 in O_2 at 800 °C

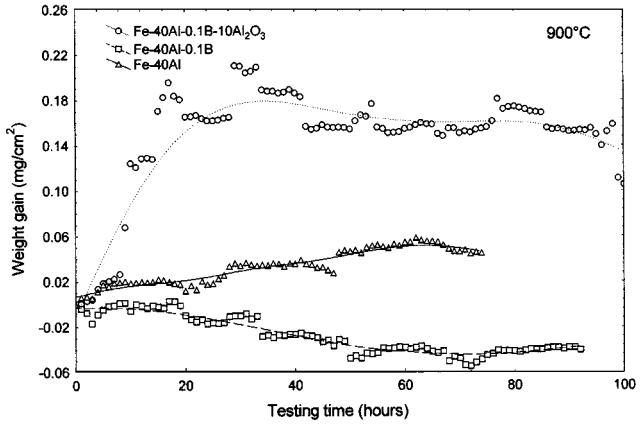

Fig. 2 Gravimetric curves for isothermal oxidation of Fe40Al, Fe40Al + B, and Fe40Al + B + Al_2O_3 in O_2 at 900 °C

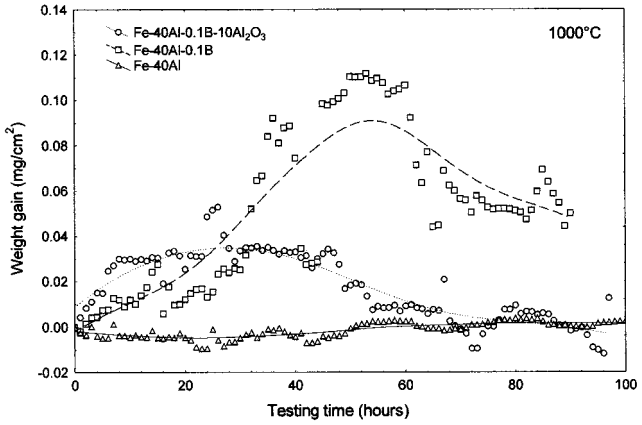

Fig. 3 Gravimetric curves for isothermal oxidation of Fe40Al, Fe40Al + B, and Fe40Al + B + Al_2O_3 in O_2 at 1000 °C

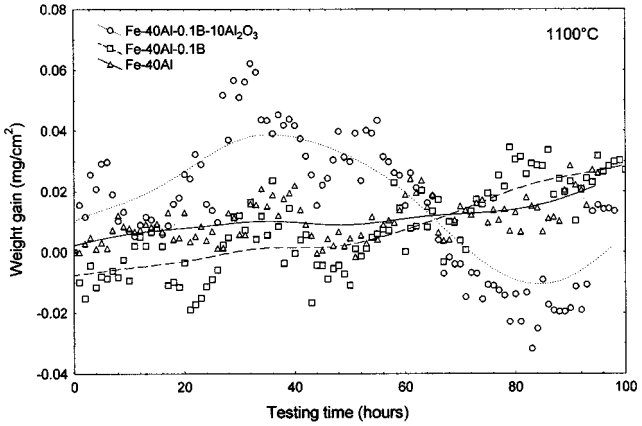

Fig. 4 Gravimetric curves for isothermal oxidation of Fe40Al, Fe40Al + B, and Fe40Al + B + Al_2O_3 in O_2 at 1100 °C

microalloying constituent. The reinforcement phase was commercially pure (99.99%) single-crystal α-alumina platelets with an average diameter of 3 μm. The synthesis of the FeAl alloys and experimental variables used for spray atomization and deposition are described elsewere.[9]

Weight-gain experiments were performed in oxygen at 800, 900, 1000, and 1100 °C in a thermobalance controlled by a desk-top computer. Specimens measuring 6 × 6 × 2 mm were used. Prior to use, the specimens were ground to 600 grade emery paper, washed, and degreased with acetone. The tests lasted 100 h. The experiments were supported by electron microscopy and x-ray diffraction studies.

3. Results and Discussion

The weight-gain data for the three intermetallic materials at different temperatures are given in Fig. 1 through 4. The 800 °C curve shows moderate weight gains of 0.1 mg/cm^2 for the Al_2O_3 containing intermetallic material after 100 h, with no obvious signs of scale spallation. However, the Fe40Al and the 0.1B alloys show some weight loss due to spalling, which was observed in the form of an extremely fine dust. Oxidation at 900 °C also produced some signs of scale spalling on the same alloys, but at that temperature, the Al_2O_3-containing alloy had the highest weight gain, about 0.22 mg/cm^2. It is important to note that at these two temperatures, the 0.1B alloy showed the lowest weight gain and it had negative slopes in the weight-gain curves from the very beginning.

At 1000 and 1100 °C, the three alloys exhibited signs of scale spalling (Fig. 3 and 4). At 1000 °C, the alloy that had the lowest weight gain and scale spalling, with a negative slope from the begining, was Fe40Al. The B and the Al_2O_3 started to lose weight after 40 and 50 h, respectively, which appeared on the surface specimen as a very fine dust, but the B-containing alloy had the highest weight gain this time. At 1100 °C, this weight loss was much more evident, since the weight-gain curves were much more erratic, having combined positive slopes in the weight-gain curves. It is important to note that, with the exception of the 800 °C data, as the temperature increased, the maximum weight gained for the different alloys decreased.

The scale phases produced are mosly Al_2O_3 with some iron oxides such as Fe_2O_3 and Fe_3O_4, as can be seen in Fig. 5

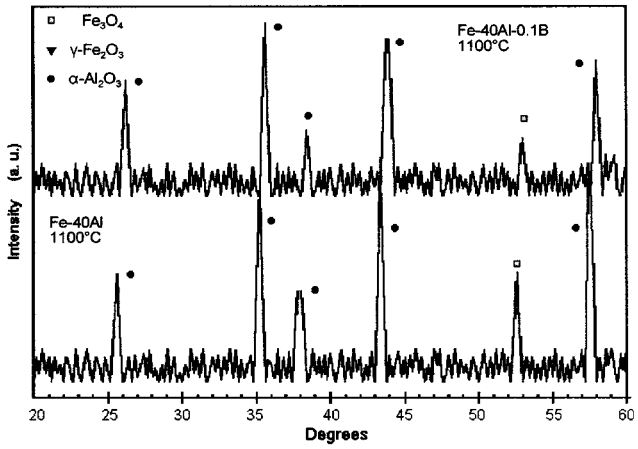

Fig. 5 Scale phases found with x-ray diffraction after isothermal oxidation of Fe40Al and Fe40Al + B at 1100 °C

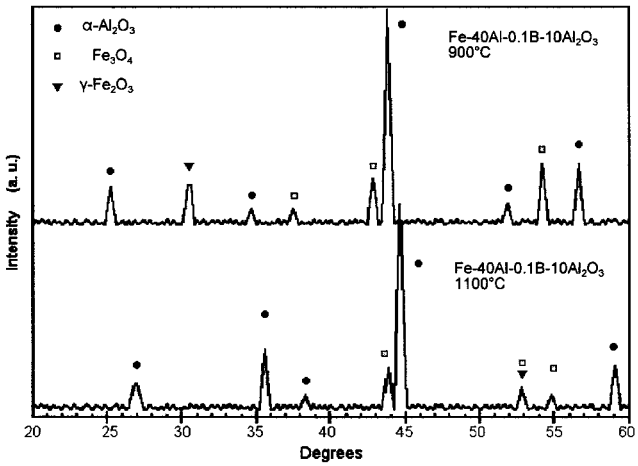

Fig. 6 Scale phases found with x-ray diffraction after isothermal oxidation of Fe40Al + B + Al_2O_3 at 900 and 1100 °C

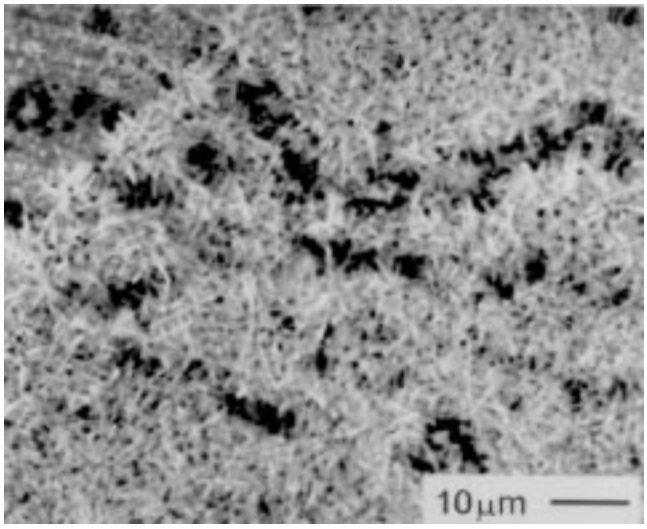

Fig. 7 Morphology of the external oxide of Fe40Al + B + Al_2O_3 oxidized at 800 °C in O_2

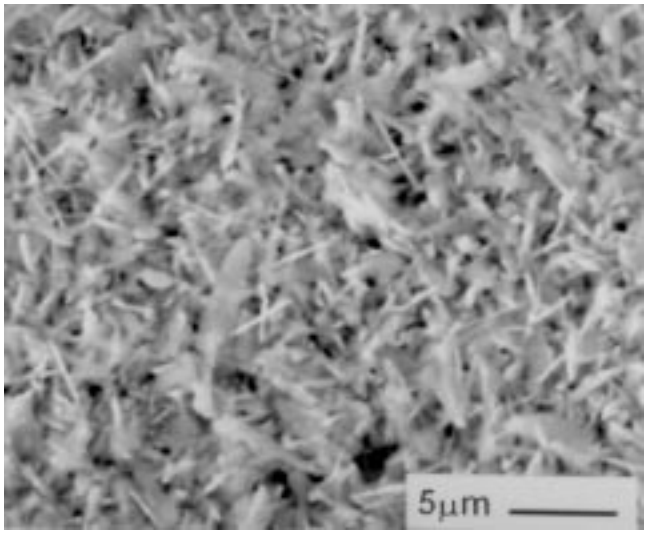

Fig. 8 Morphology of the external oxide of Fe40Al oxidized at 900 °C in O_2

and 6. Smialek,[3] studying the oxidation of Fe40 (at.%) Al containing 1Hf and 0.4B, found α- and θ-Al_2O_3 at 900 °C, and mostly α-Al_2O_3 with a lesser amount of θ-Al_2O_3 at 1000 and 1100 °C. The predominant surface product that forms on iron aluminides between 600 and 800 °C has been reported to be γ-Al_2O_3,[10] but it is also possible for θ-Al_2O_3 or other forms of alumina to exist in this temperature range.[11] At higher temperatures, α-Al_2O_3 is the principal steady-state protective product.[11] The θ-Al_2O_3 is a fast-growing transition alumina, whereas α-Al_2O_3 is a slower growing, more compact type of alumina, which appears to start around 900 °C, and typically is not observed below this temperature; however, the others types of alumina observed below 900 °C do provide corrosion and oxidation resistance, but less than this type of alumina.

Below 900 °C, the three alloys formed whisker morphologies with shallow depressions on the scale microstructures (Fig. 7 and 8). Such scales have also been observed for 900 °C oxidation of Fe40Al + 1Hf[3] and the 900 °C oxidation of Ni50Al + 0.1Zr under the same conditions.[12] In both cases, the whisker morphology was associated with a fast-growing transition θ-Al_2O_3. Examination of a cross section of the oxidized Fe40Al specimen at 900 °C revealed some porosity in the metal-oxide interface (Fig. 9). This porosity could be the cause of scale spallation. Severe spalling to bare metal due to interfacial voiding has also been observed in the 900 °C isothermal oxidation of Fe40Al + 1Hf[3] and Fe40Al + 0.1Zr + 0.4B. It was also observed in the 1100 °C isothermal oxidation of Ni40Al alloy,[12] but nevertheless this alloy maintained good cyclic oxidation resistance at 1100 °C. Isothermal oxidation also produced spalling to bare metal for a 0.1Zr-doped Ni50Al due to interfacial voidage, but only above 1300 °C.[12]

Oxidation at 1000 °C produced spheroidization and coarsening of any whisker morphology in the three alloys, as can be seen in Fig. 10. Oxidation at 1100 °C produced tremendous

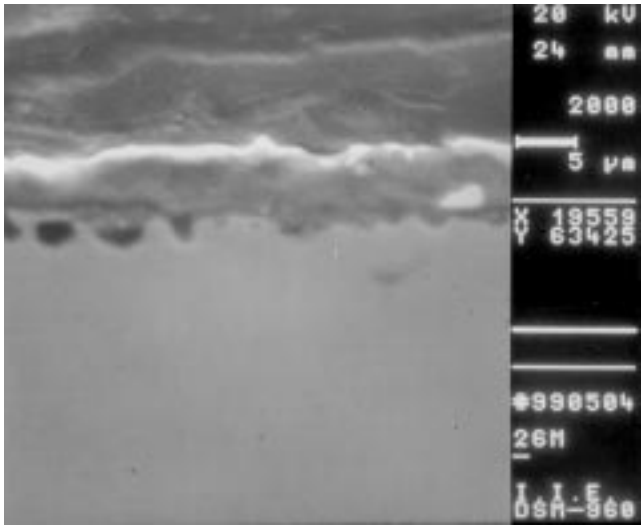

Fig. 9 Cross section of the metal-oxide interface of Fe40Al oxidized at 900 °C in O_2

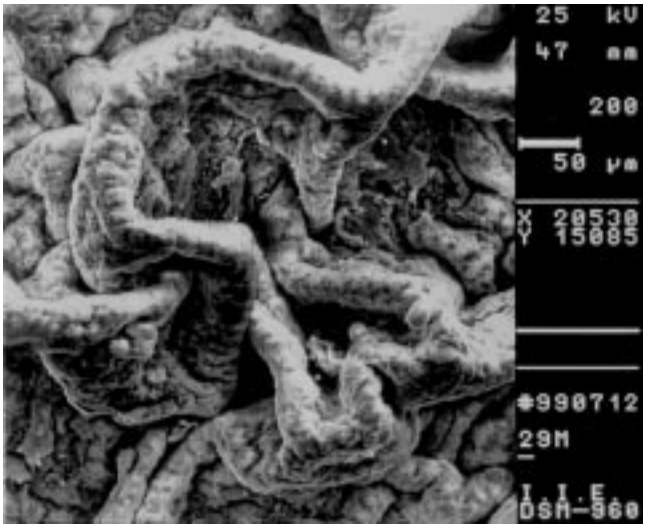

Fig. 11 Morphology of the external oxide of Fe40Al oxidized at 1100 °C in O_2

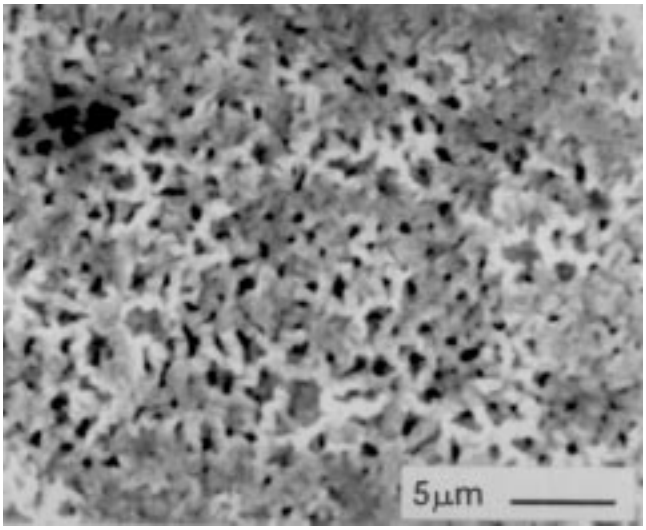

Fig. 10 Morphology of the external oxide of Fe40Al + B oxidized at 1000 °C in O_2

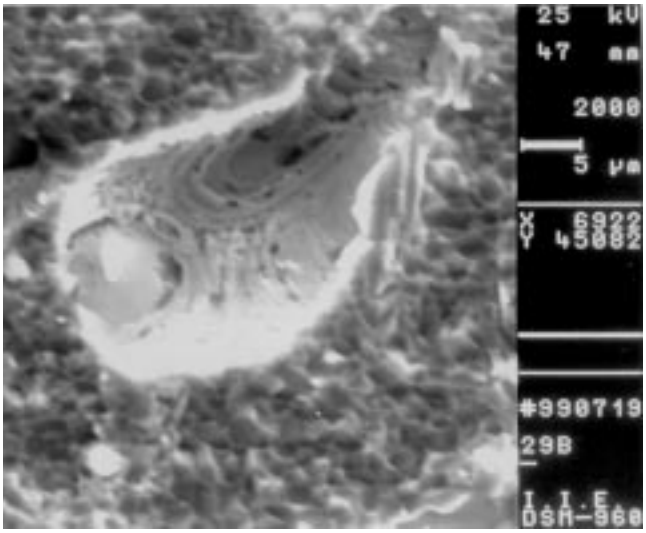

Fig. 12 Morphology of the external oxide of Fe40Al + B oxidized at 1100 °C in O_2

wrinkling, cracking, and spalling of the Fe40Al alloy (Fig. 11). This damage explains the decidedly downward trend in weight change in Fig. 3 and 4. Another possible explanation is the presence of trace amounts of Fe_2O_3 and Fe_3O_4. Further coarsening took place in the Fe40Al + 0.1B alloy (Fig. 12) and the Fe40Al + 0.1B + 10Al_2O_3 alloy (Fig. 13) and the cells were flattened and occupied the majority of the surface.

The scale adhesion of iron aluminides is affected by the segregation of sulfur to the scale-alloy interface, the presence of reactive elements (RE) in the alloy, interfacial and scale defects (such as voids), and alloy strength.[13] Specifically, Hou *et al*. show that additions of 0.1 (at.%) Zr to Fe28Al-5Cr avoided sulfur segregation at the interface when oxidized at 1000 °C and the scale spallation[14] was lowered. The presence of RE such as Zr, HfO_2, or Y_2O_3 in iron aluminides, either as alloying elements or oxide dispersoids, leads to the development of an alumina scale with a primarily columnar grain structure (Fig. 14) that is quite distinct from the large equiaxed grains of the Al_2O_3 and that grows without the RE. These columnar grains were observed at 900 °C for the Fe40Al + 0.1B alloy, are characteristic of alumina formers with alloying elements with additions that are effective in promoting scale adherence, and occur with the transport of RE ions to the oxide-metal interface and through the scale.[13]

Another factor that affects the scale adhesion is the greater propensity for interfacial void formation associated with oxidation of some iron aluminides as compared with other alumina formers. These voids were observed on the Fe40Al oxidized at 900 °C (Fig. 9)and this will lead, probably, to a more rapid scale failure and spallation.

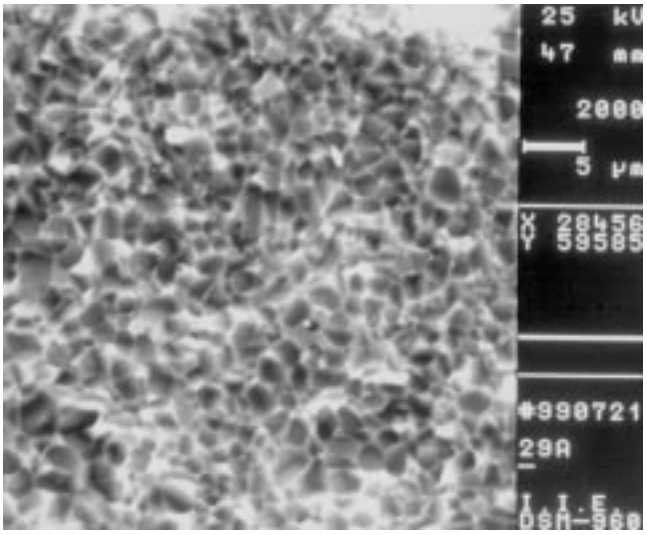

Fig. 13 Morphology of the external oxide of Fe40Al + B + Al_2O_3 oxidized at 1100 °C in O_2

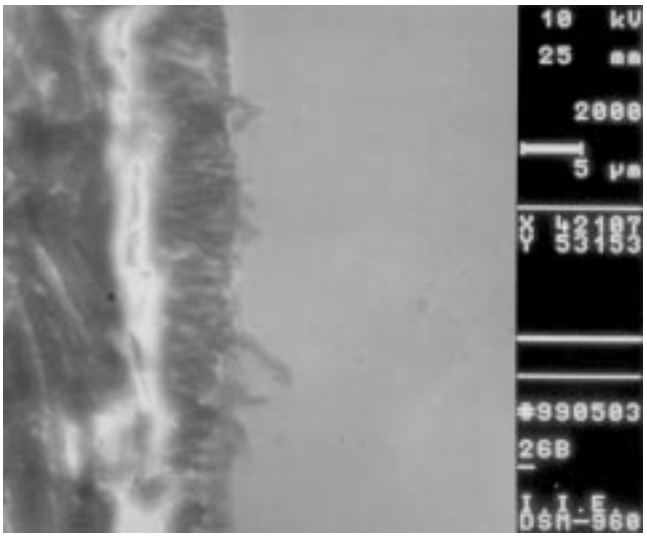

Fig. 14 Cross section of the metal-oxide interface of Fe40Al + B oxidized at 800 °C in O_2

4. Conclusions

In general terms, it can be said that the three alloys showed excellent oxidation resistance, although in most cases, the main problem was some scale spalling, especially at 1100 °C. At 800 and 900 °C, the Fe40Al + 0.1B alloy had the lowest weight gain, whereas the Fe40Al alloy had the highest weight gain at 800 °C and the Fe40Al + 0.1B + $10Al_2O_3$ alloy was the least oxidation resistant at 900 °C. At 1000 °C, the Fe40Al + 0.1B alloy showed the highest weight gain with 0.12 mg/cm^2 and the Fe40Al alloy the lowest. At 1100 °C, the Fe40Al alloy was the least resistant, whereas the Fe40Al + 0.1B alloy performed the best, but the three alloys exhibited a paralinear bahavior on the weight-gain curves, indicating the spalling, breaking down, and rehealing of the oxides. The main phases found in the scales were α-Al_2O_3 with some iron oxides such as Fe_2O_3 and Fe_3O_4. The spalling of the alloys was discussed in terms of voids formed at the metal-oxide interface, segregation of impurities, and the substrate strength.

References

1. C. Sykes and J. Bampfylde: *J. Iron Steel Inst.*, 1934, vol. 130, pp. 389-418.
2. G. Webband and A. Lefort: *Symp. Proc. Fatigue and Fracture of Ordered Intermetallic Materials: I*, TMS, Warrandale, PA, 1994, p. 103.
3. J.L. Smialek, J. Doychak, and D.J. Gaydosh: in *Oxidation of High-Temperature Intermetallics*, T. Grobstein and J. Doychak, eds., TMS, Warrandale, PA, 1989, p. 83.
4. J.H. Schneibel: *Mater. Sci. Eng.*, 1992, vol. A153, p. 684.
5. S. Zeng, X.R. Nutt, and E.J. Lavernia: *Metall. Mater. Trans.*, 1994, vol. A26, p. 817.
6. R.G. Baligidad, U. Prakash, and A. Radha Krishna: *Mater. Sci. Eng.*, 1997, vol. A230, p. 188.
7. B.A. Pint, P.F. Tortorellli, and I.G. Wright: *Mater. Corr.*, 1996, vol. 47, pp. 663-74.
8. B.A. Pint, P.F. Tortorellli, and I.G. Wright: *Mater. High Temp.*, 1997, vol. 15, p. 613.
9. L. Martinez, O. Florez, M. Amaya, A. Duncan, S. Viswanathan, and D. Lawrynowics: *J. Mater. Synth. Processing*, 1997, vol. 5, p. 65.
10. M. Sakiyama, P. Tomasewicz, and G.R. Wallwork: *Oxid. Met.*, 1979, vol. 13, pp. 573-77.
11. B.A. Pint: in *Fundamental Aspects of High Temperature Corrosion*, D.A. Shores, R.A. Rapp, and P.Y. Hou, eds., The Electrochemical Society, Pennington, NJ, 1997, pp. 74-85.
12. R.A. Perkins, G.H. Meier, and K.T. Chiang: Paper presented at the *Workshop on Oxidation of High Temperature Intermetallics*, sponsored by NASA Lewis Research Center, Case Western Reserve University, and the Cleveland Chapter of AIME, Cleveland, OH, Sept. 22–23, 1988.
13. P.F. Tortorelli and K. Natesan: *Mater. Sci. Eng.*, 1998, vol. A258, pp. 115-25.
14. P.Y. You: in *Microscopy of Oxidation*, S.B. Newcomb and J.A. Little, eds., Institute of Materials, London, 1997, pp. 140-49.